

Experimental Collimation of Cerenkov SHG Blue Laser Beam with a Cylindric Mirror

Ming WANG*

Osami WADA†

Ryuji KOGA†

(Received October 2, 1995)

SYNOPSIS

A cylindric mirror was used, in place of a parabolic mirror, to collimate the crescent blue laser beam radiated from the Cerenkov SHG in channel waveguide configuration. The cylindric mirror radius is requested to be twice the focal length of the parabolic mirror. The focusing effect of the cylindric mirror in collimation can be compensated by slightly lifting the mirror in its normal direction. Under the condition that the mirror was declined by 5.56° and lifted by $25 \mu\text{m}$, we got the collimated beam with divergence angle less than 1.3 mrad. In the focusing experiment, the collimated beam was focused with spotsizes of $1.8 \mu\text{m}$. The details on the analysis and experiment are reported.

1. INTRODUCTION

To collimate the crescent blue laser beam radiated from the Cerenkov SHG in channel waveguide configuration^[1~4], we proposed a convenient collimation optics using a parabolic mirror^[5,6]. In this parabolic mirror optics, the anisotropy of the optical crystal – LiNbO_3 on which the channel waveguide is fabricated by the proton exchange technique can be compensated by declining the mirror with an angle η . When the declining angle is set to be 5.5° , the optics gives the optimum collimation, i.e., the crescent beam can be collimated with the divergence less than 0.3 mrad. The collimated beam can be further focused by using an objective lens to a fine beam with spotsizes less than $1 \mu\text{m}$.

For the convenience to get in hand, a cylindric mirror can be used in place of a parabolic mirror as the collimation mirror. When a cylindric mirror is used, its radius is required to be twice the focal length of the parabolic mirror. In this case, the left problem lies in the focusing effect in collimation. This effect can be compensated by slightly lifting the mirror in its normal direction. The mirror lift is figured under the criterion of minimum wave aberration. The calculation indicates that the crescent beam can be collimated with the divergence less than 1.3 mrad.

*Graduated School of Natural Science and Technology

†Department of Electrical and Electronic Engineering

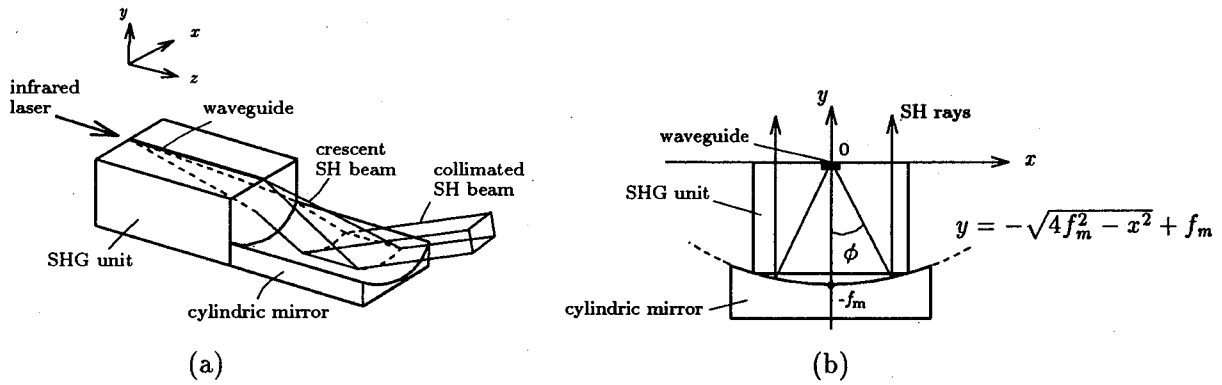


Fig.1 Cylindric mirror collimation configuration for the crescent shaped blue laser beam radiated from Cerenkov channel waveguide SHG(a). The mirror is located beside the SHG element so that its focal axis is coincident with the waveguide axis. f_m is the focal length of the mirror and ϕ is an azimuth angle indicating the range where the SH light is radiated(b).

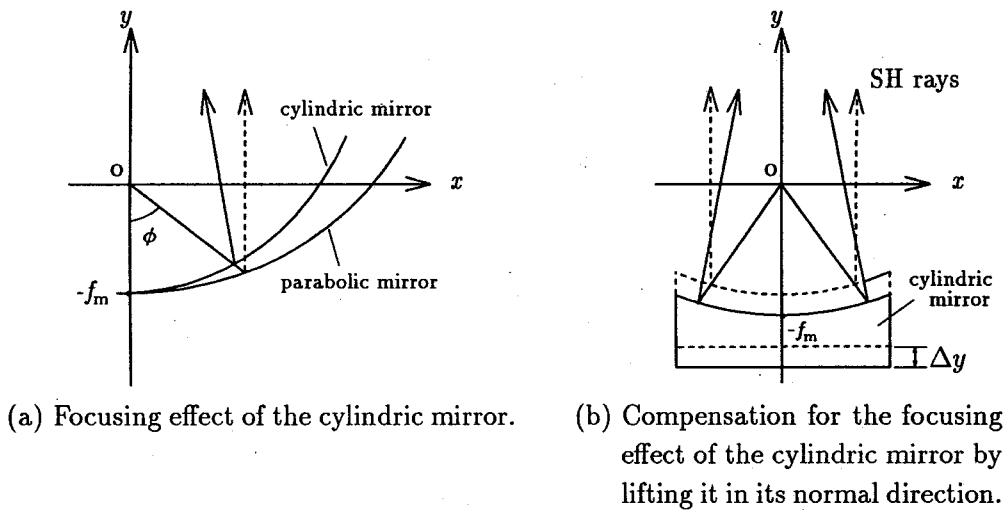


Fig.2 Comparison of the cylindric mirror optics with the parabolic mirror optics. The focusing effect of the cylindric mirror(a) can be compensated by lifting it along its normal direction(b).

In the collimation experiment, the cylindrical mirror is selected with radius of 12.98 mm, i.e., the focal length is 6.49 mm. The measured beam divergence is less than 1.3 mrad. In the focusing measurement, the multi-reflection between the source laser diode and the SHG element would cause the multimode lasing in the source laser diode. The resulting wavelength variation leads to the increase of the beam spotsize. By using an optical isolator, the multi-reflection was suppressed and the focused beam was obtained with spotsize less than 1.8 μm .

2. CRESCENT BEAM COLLIMATION BY USING A CYLINDRIC MIRROR

The cylindrical mirror collimation optics is the same in the configuration as the parabolic mirror optics^[5], as illustrated in Fig.1. To collimate the crescent beam, the cylindrical mirror is required to have the same focal length as that of the parabolic mirror. For a cylindrical mirror with radius of $2f_m$, we consider its focal length to be f_m (Fig.1-(b)). Compared with the parabolic mirror optics, an additional problem arises in the focusing effect when the crescent beam is reflected by a cylindrical mirror(Fig.2-(a)). This focusing effect appears because of the fact that the curvature radius of a cylindrical mirror is smaller than that of a parabolic mirror, particularly at the mirror edges. Thus the further apart the center of the beam rays reflected by the cylindrical mirror, the larger are the phase advances of them. Based on this point of view, we can compensate this focusing effect by slightly lifting the cylindrical mirror along its normal direction, as shown in Fig.2-(b). In this work, we apply the concept of wave aberration^[9,10] to the evaluation of the collimated beam.

2.1 Evaluation of the Collimated Beam

It is known that a beam suffers degradation in intensity while it passes through an optical system with aberrations. This kind of degradation is usually evaluated by a ratio of the peak intensity degraded to that not degraded, i.e., *Strehl Definition*(SD):

$$SD = 1 - \left(\frac{2\pi}{\lambda}\right)^2 \langle \Delta W_a^2 \rangle = 1 - \left(\frac{2\pi}{\lambda}\right)^2 s^2 \quad (1)$$

where λ is the wavelength and W_a the wavefront aberration; $\langle \rangle$ represents the statistical mean, ΔW_a the deviation and $\langle \Delta W_a^2 \rangle = s^2$ the variance.

For different types of beam profile, S. Szapiel introduced the concept of weighted variance of wavefronts^[9]. In Cerenkov SHG in channel waveguide configuration, the SH beam has an irregular intensity profile even after being collimated^[5,6]. Because the aberrations over a region where beam intensity is stronger dominate the beam quality, we here weight the aberration with beam intensity I in the statistical mean and variance of the aberrations as:

$$\langle W_a \rangle = \frac{\iint_S I W_a dx dy}{\iint_S I dx dy}, \quad (2)$$

$$s^2 = \frac{\iint_S I (W_a - \langle W_a \rangle)^2 dx dy}{\iint_S I dx dy}. \quad (3)$$

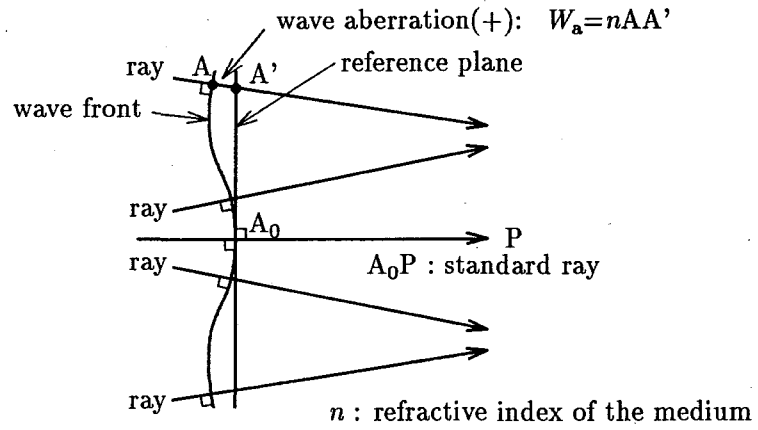


Fig.3 Concept of aberration evaluation of a collimated beam. The reference for a collimated beam is assumed to be a plane.

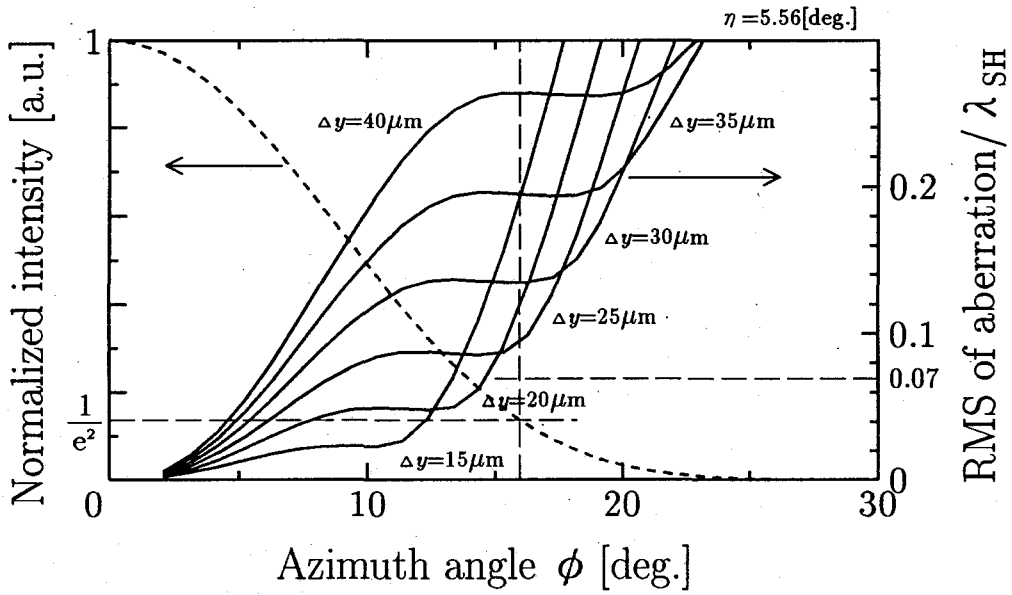


Fig.4 Aberration of the SH beam reflected by the cylindric mirror with different mirror lift values. The declining angle η for compensating the anisotropy of LiNbO_3 was set to be 5.56° .

The intensity weighted standard deviation s redefined above is alternatively referred to as RMS(Root Mean Square) here. To calculate this RMS, we take a plane as the reference[†], different from the usual spherical reference, shown in Fig.3 where the deviation of the wavefront from the reference plane is defined as the aberration.

The phase profiles of the beam reflected by the cylindric mirror with different values of the declining angle η ^[5] and the lift in mirror's normal direction Δy were calculated by using the ray tracing method^[11]. In the calculation, the SH beam rays are traced when they are radiated from the waveguide till they reach at the cylindric mirror. The mirror's focal length f_m and the SHG element parameters used in the calculation are the same as those listed in Table I. The calculated RMS is shown in Fig.4. If the mirror is lifted by 25 μm in its normal direction, the RMS of the wave aberration is obtained to be 0.1 λ_{sh} over the region where the normalized beam intensity holds on a level not less than $\exp(-2)$. If we consider over a region where the beam power more than 87%^{††} is included, the RMS is only 0.06 λ_{sh} , less than Marechal's Criterion 0.07 λ_{sh} ^[10].

For these parameters, the collimated beam width defined as the full width at $\exp(-2)$ of the peak intensity was calculated by using the ray tracing method and the integral theorem of Kirchhoff. A virtual aperture plane was set 200 mm away from the mirror for the integral. The calculated result is shown in Fig.5, which gives the divergence of the collimated beam less than 1.3 mrad.

2.2 Focusing of the Collimated Beam

The collimated beam can be focused by using an objective lens. For a lens with focal length of 5.3 mm and the numerical aperture 0.65, the calculated focusing is given in Fig.6. The sidelobes in x direction results from the advanced phase profile in the edges of the cylindric mirror. The minimum spotsize in x direction is 1.18 μm (mainlobe) and that in y direction is 1.04 μm . By the way, in the parabolic mirror collimation optics, the same focusing gives a beam spotsize of 0.91 μm and 0.86 μm , respectively in x direction and y direction.

3. EXAMINATION OF COLLIMATION ACHIEVEMENT

The crescent beam collimation was measured in the set up shown in Fig.7. The specifications of the devices used in this measuring system were listed in Table I. When the infrared beam(830 μm) from a laser diode is injected into the Cerenkov SHG element, the second harmonic blue laser beam is radiated in a crescent shape from the element. This crescent blue beam is collimated by the cylindric mirror. The collimated beam profile is taken by a CCD camera and stored in a personal computer. Photos of the crescent blue beam and the collimated beam are illustrated in Fig.8. The crescent beam was projected to a white paper plate and the image was taken by a camera. The collimated beam photo was taken from the monitor screen.

[†]Following from the geometrical optics, the wavefront of a perfectly collimated beam is considered to be a plane(the divergence being zero or the curvature radius being infinite).

^{††}For a beam with Gaussian profile, 87% of the total beam power is included over a region where the normalized beam intensity $\geq \exp(-2)$.

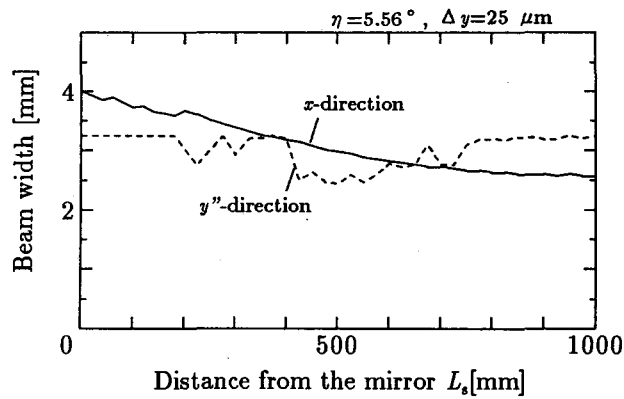


Fig.5 Beam width defined as the full width at $\exp(-2)$ of the peak intensity, with distance L_s from the mirror at η 5.56°. Divergence of the collimated beam is less than 1.3 mrad.

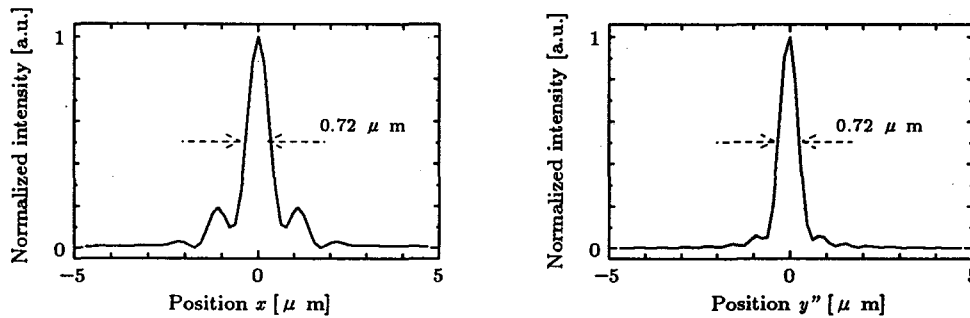


Fig.6 Spotsize of the focused beam by using an objective lens set at 100 mm away from the mirror. The focal length of the lens is 5.3 mm and the numerical aperture 0.65. The beam spotsize in x direction is $1.18 \mu\text{m}$ (mainlobe), and that in y'' direction is $1.04 \mu\text{m}$. The FWHM is $0.72 \mu\text{m}$.

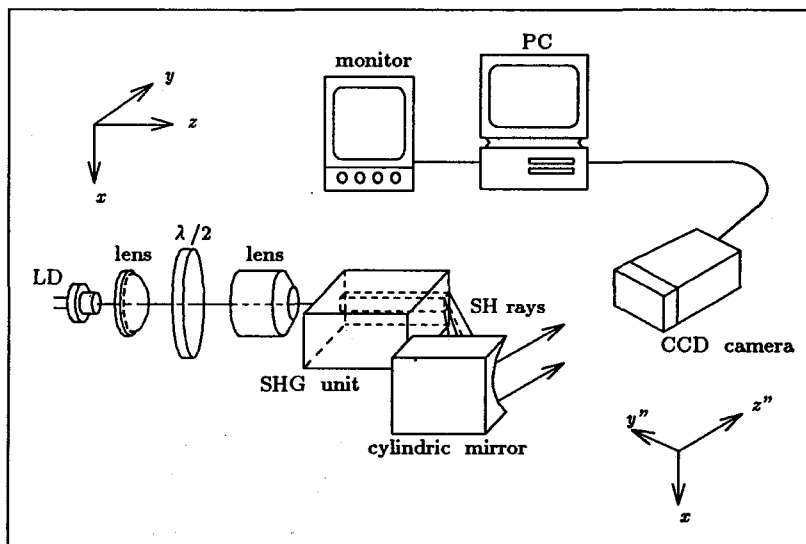
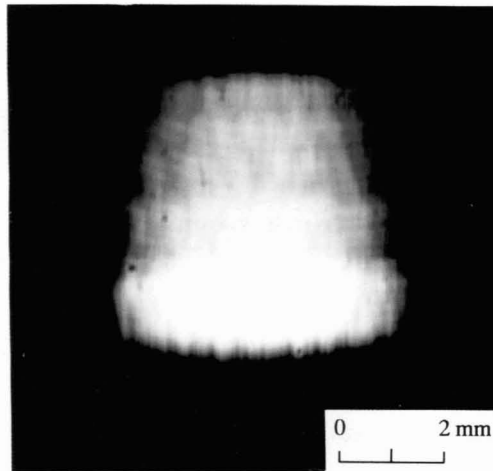


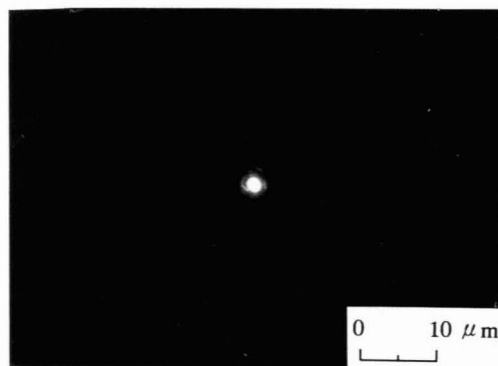
Fig.7 Measuring system for the collimation.



(a) Photo of the crescent blue beam radiated from the channel waveguide Cerenkov SHG element, taken from a white paper plate.



(b) Photo of the collimated beam, taken from the monitor screen(Fig.7).



(c) Photo of the focused, taken from the monitor screen.

Fig.8 Photos of the crescent blue laser beam(a), collimated beam(b) and the focused beam(c).

Table I: Specifications of the devices used in collimation and focusing.

Device		Type	Specification
Laser diode		Sharp LT015MD	wavelength: 830 nm mode interval: 0.33 nm
SHG element	substrate	LiNbO ₃	length: 18 mm width: 5 mm thickness: 6 mm
	waveguide	proton exchanged	length: 18 mm width: 2 μm thickness: 0.4 μm
Cylindric mirror		SIGMA KOKI TCCA-1515-12.98	radius: 12.98 mm (focal length f_m : 6.49 mm)
Focusing lens		Nikon objective lens CF M plan 40 DIC	focal length: 5.3 mm N.A.: 0.65

To evaluate collimated beam, the beam spotsizes in different propagation distances were taken and are shown in Fig.9. From this figure, we get the the divergence less than 1.3 mrad. This divergence is quite less than that got in a conic lens collimation optics^[8].

4. FOCUSING MEASUREMENT AND EFFECT OF MULTIREFLECTION

After the crescent beam was collimated with divergence less than 1.3 mrad., we focused it further by using an objective lens(the specification is listed in Table I). One of the results is shown in Fig.10. In collimation direction, i.e., in x direction, the beam spotsize is more than 5 μm , and that in y direction is more than 30 μm . We consider that this phenomena is due to the multimode lasing caused by the returned light(optical feedback) to the source laser diode. Saying in detail, when the laser beam is injected into the waveguide of the Cerenkov SHG element, some part of the incident light will be reflected. This reflected light enters into the source laser diode and causes the multimode lasing. The multimode lasing is equivalent to the large variation in wavelength, which results in the variation of the Cerenkov angle^[5], and eventually in the deflection of the collimated beam(Fig.11). According to the spectrum in multimode lasing got by an optical spectrum analyzer(Antitsu MS9701C), the wavelength variation between two adjacent modes is about 0.33 nm(Fig.12). A simple geometric optical evaluation reveals that for the wavelength variation of 0.33 nm, the corresponding deflection of the focused beam is about 2 μm . This can be observed in Fig.10.

To suppress the returned light, we inserted an optical isolator between the source laser diode and the SHG element. Then the multimode lasing disappeared. Under this condition, the beam focusing was carried out successfully. The result is illustrated in Fig.13. The spotsize in the beam collimation direction, i.e., in x direction is 1.7 μm , and that in y direction is 1.8 μm (the FWHMs both in x and y directions are less than 1.0 μm), about 1.4 times of the analytical result.

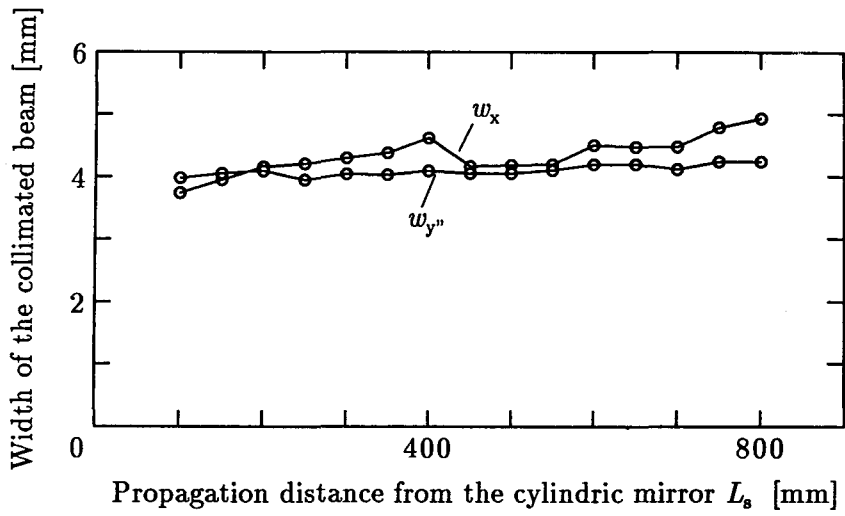


Fig.9 Measured beam spotsize defined as the full width at $\exp(-2)$ of the peak, with distance L_s from the cylindric mirror The divergence of the collimated beam is less than 1.3 mrad.

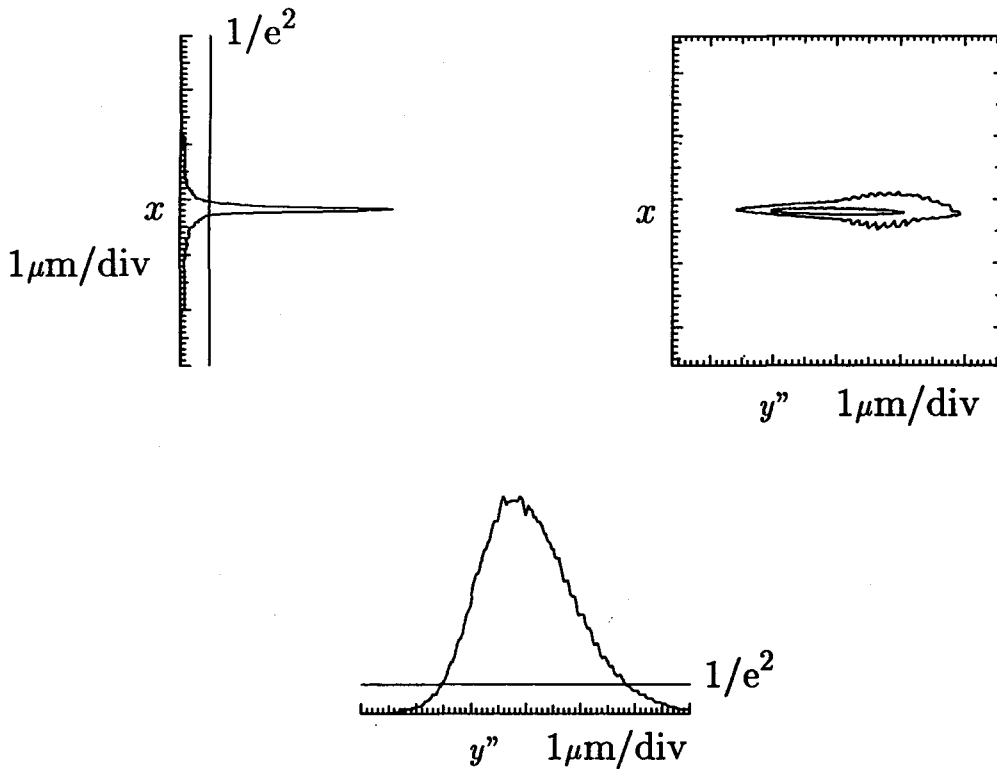


Fig.10 Measured profile of the beam focused by an objective lens without optical isolator used. Because of the multimode lasing in the source laser, the beam was not be focused finely.

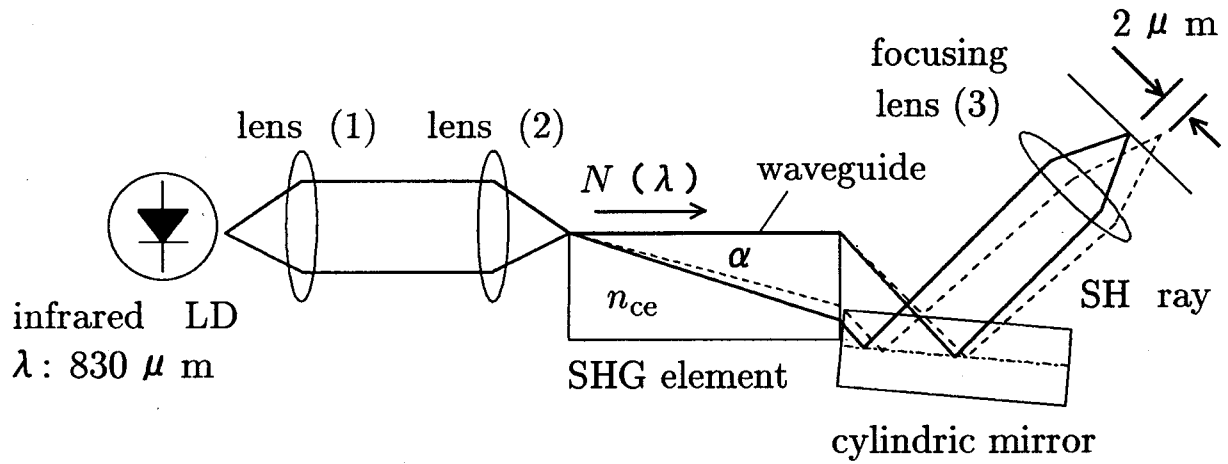


Fig.11 Multireflection between the laser diode and the SHG element and the deflection of the collimated beam due to the multimode lasing. According to the geometric evaluation, the beam deflection for a mode interval is about $2 \mu\text{m}$.

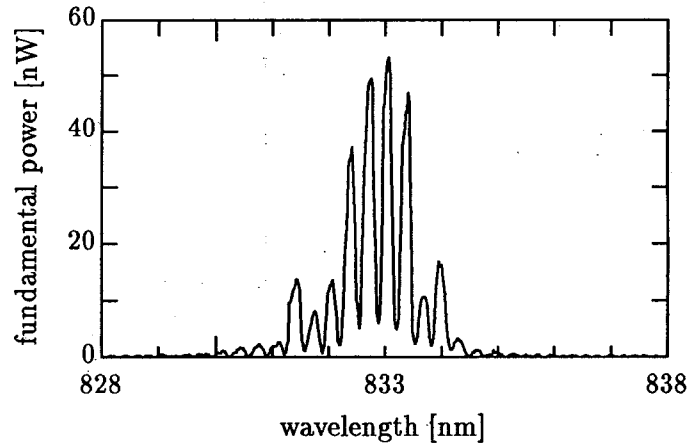


Fig.12 Spectrum of the source laser diode in multimode lasing caused by multireflection between the laser diode and the SHG element. The mode interval is about $0.33 \mu\text{m}$.

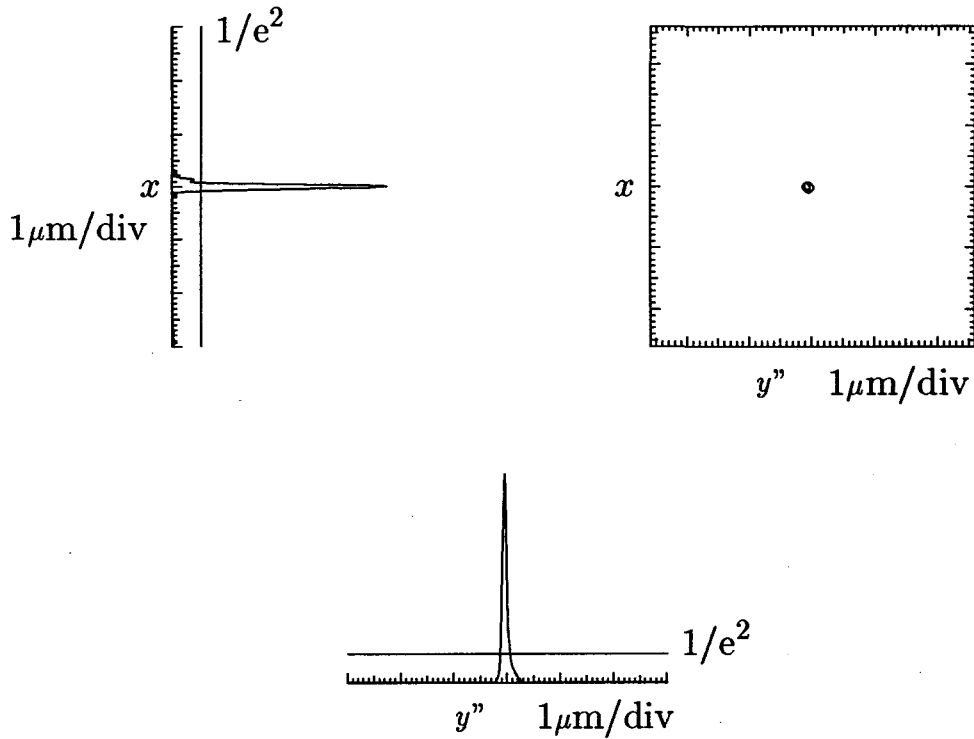


Fig.13 Measured profile of the beam finely focused by an objective lens with an optical isolator used. The spotsize defined as full width at $\exp(-2)$ of the peak level is $1.8 \mu\text{m}$, and that in y'' direction is $1.7 \mu\text{m}$.

5. CONCLUSION

A cylindric mirror was used in place of a parabolic mirror to collimated the crescent shaped blue laser beam radiated from the channel waveguide Cerenkov SHG. The measured divergence angle of the collimated beam shows a good agreement with the analytical result. The collimation condition was obtained through the same mechanism as the parabolic mirror optics. Because the curvature radius of the cylindric mirror is less than that of a parabolic mirror, there arises a problem of focusing effect in collimation when a cylindrical mirror is used. This effect can be compensated for by slightly lifting the mirror in its normal direction. The analytical and measured collimation and focusing of a cylindric mirror optics were listed in Table II, to which the analytical collimation and focusing of a parabolic mirror optics were added for the comparison.

REFERENCES

- [1] G. Tohmon *et al*, SPIE-Int. Soc. Opt. Eng., 898(1988), Miniature Optics and Lasers, pp.70-75.
- [2] T. Taniuchi, *et al*, SPIE-Int. Soc. Opt. Eng., 864(1988), Advanced Optoelectronic Technology, pp.36-41.

Table II: Collimation and focusing in cylindric mirror optics and parabolic mirror optics

Mirror type		Parabolic	Cylindric
η		$5.52^\circ \sim 5.58^\circ$	5.56°
Δy		0	$20 \sim 30 \mu\text{m}$
RMS	included power $\geq 90\%$	$0.04\lambda_{\text{sh}}$ ($\eta = 5.58^\circ$)	$0.05\lambda_{\text{sh}}$ ($\eta = 5.56^\circ, \Delta y = 20\mu\text{m}$)
	normalized intensity $\geq \exp(-2)$	$0.06\lambda_{\text{sh}}$ ($\eta = 5.56^\circ$)	$0.09\lambda_{\text{sh}}$ ($\eta = 5.56^\circ, \Delta y = 25\mu\text{m}$)
Divergence	Calculated	0.3 mrad.	1.3 mrad.
	Measured		1.3 mrad.
Spotsize of focused beam	Diffraction limited	$0.74\mu\text{m} \times 0.88\mu\text{m}$	$0.94\mu\text{m} \times 0.88\mu\text{m}$
	Calculated	$0.90\mu\text{m} \times 0.86\mu\text{m}$	$1.18\mu\text{m} \times 1.04\mu\text{m}$
	Measured		$1.70\mu\text{m} \times 1.80\mu\text{m}$

- [3] K. Mizuuchi, *et al*, Appl. Phys. Lett., 58, 24(1991), pp.2732-2734.
- [4] K. Yamamoto, *et al.*, J. Appl. Phys., 70, 11(1991), pp.6663-6668.
- [5] M. Wang, *et al.*, Memoirs of the Faculty of Eng., Okayama Univ., 28, 2(1994), pp.33-44.
- [6] M. Wang, *et al.*, SPIE-Int. Soc. Opt. Eng., 2321(1994), Optoelectronic Science and Engineering, pp.196-199.
- [7] G. Hatakoshi, *et al.*, Opt. Lett., 15, 23(1990), pp.1336-1338.
- [8] K. Tatsuno, *et al.*, Appl. Opt., 31, 3(1992), pp.305-310.
- [9] D. D. Lowenthal, Appl. Opt., 13, 9(1974), pp.2126-2133.
- [10] S. Szapiel, J. Opt., Soc. Am., 72, 7(1982), pp.947-956.
- [11] Q. Liang, Appl. Opt., 29, 7(1990), pp.1008-1010.